CHIMESE JOURNAL OF GEOCHEMISTRY Vol. 26 No. 1 2007

DOI: 10.1007/s11631-007-0098-3

Refinement of a lunar FeO mapping method

LIU Jian (刘剑)[1,2*], OUYANG Ziyuan (欧阳自远)[1], LI Chunlai (李春来)[3], and ZOU Yongliao (邹永廖)[3]

[1] *Institute of Geochemistry, Chinese Academy of Sciences, Guiyang 550002, China*

[2] *Graduate School of Chinese Academy of Sciences, Beijing 100039, China*

[3] *National Astronomical Observatories, Chinese Academy of Sciences, Beijing 100012, China*

** Corresponding author, E-mail: liuj@bao.ac.cn*

Received December 2, 2005; accepted February 28, 2006

Abstract Clementine UVVIS and NIR data from the lunar sampling sites (totaling 46 sampling sites) were processed and used to refine the iron determination method of Le Mouéic et al. (2000, 2002). We found that about 21 sampling sites are unsuitable to Le Mouéic et al's spectral parameters ("slope" and "depth l") because their 1500 nm filter could not be used as spectral parameters' right shoulders and to evaluate the depth of the 1-μm absorption feature accurately. We used the rest 25 sampling sites to refine the method developed by Le Mouéic et al. (2000, 2002) and obtained our own equation of FeO content determination. We tested our own equation, and the results are satifactory. In our work we also acquired some useful experiences in scientific applications of our own dataset of the Chang'E-1 mission.

Key words Moon; spectrum; mineral

1 Introduction

Chang'E-1 mission, the first of a series of Chinese missions to the Moon，is brought into effect. One of its scientific objectives is to analyze the abundances of elements and the distributions of surface materials on the Moon. Fourier Transform Imaging Spectrometer, the principal payload of the mission, is entitled to accomplish the objective. The payload's spectral range covers from VIS to NIR, which represents the important mineralogical characteristics of the lunar material (Xu Tao et al., 2005).

Iron is one of the most important elements which are useful for the study of the origin and evolution of the Moon because there is an extremely high inverse correlation between the abundance of iron and aluminum in the lunar samples (Haskin and Warren, 1991) and aluminum commonly used to constrain the origin and evolution of the Moon (Taylor, 1987). Owing to the importance of iron on the lunar surface, many successful efforts have been made to develop quantitative geochemical information on iron from the remote spectral reflectance data. Many scientific workers have established their own empirical relationships between the spectral properties and the abundance of iron to determine iron concentrations. Fischer and Pieters (1994, 1996) established several methods for deriving FeO for lunar highland soils. The first global map of lunar iron was derived by Lucey et al. (1995), depending on lunar samples compiled from the literature and Clementine UVVIS data, and then the mapping techniques were improved by Lucey and his coworkers (Lucey et al., 1995, 1998a, b, 2000a, b; Blewett et al., 1997). Shkuratov et al. (1999) developed a method to determine iron, titanium and the degree of maturity from a set of Earth-based telescope data. Shkuratov et al. (2003) put forward another approach based on statistical analysis of the spectral and compositional data for Apollo and Luna samples and Clementine UVVIS data to estimate and determine the abundances of FeO.

All the techniques mentioned above are based on the lunar samples' data, Clementine UVVIS data and Earth-based telescope data to estimate and determine the abundances of FeO. Le Mouéic et al. (2000, 2002) developed a new iron-abundance mapping technique in combination of the Clementine UVVIS and NIR data with lunar samples' data. The technique makes use of the spectral ratios and avoids the influence of lunar topography. However, owing to a large varying dark frame signal and uncertainties on gain and offset values (Lucey et al., 1997, 1998a, b), the Clementine NIR data set's production has been delayed. When Le Mouéic et al. (2000, 2002) undertook this piece of work, the global dataset of Clementine NIR camera still was not released. They only did some calibrations

to the local data from the Aristarchus plateau and Tycho crater, and then used the data to study the new FeO technique.

In this paper, we used the Clementine UVVIS data and NIR data from the lunar sampling sites (totaling 46 sampling sites) to refine the iron-determination method of Le Mouéic et al. (2000, 2002). This work could also acquire some useful experiences in scientific applications of the dataset of the Chang'E-1 mission.

2 Spectral theory of and spectral parameters for lunar soil

2.1 Spectral theory of lunar soil

The reflectance of lunar soil is constrained mainly by the composition of lunar soil and by the important optical effects of space weathering processes. However, exploiting the mineralogical and chemical compositions of lunar soil in terms of its spectra has been hampered by the optical effects of space weathering processes, which include the bombardment of the lunar surface by micrometeorites, solar wind ions and cosmic rays (McKay et al., 1991). The space weathering processes made the mean grain size reduced (McKay et al., 1974), produced submicroscopic single-domain iron (Hapke et al., 1975) and created amorphous coatings on individual grains (Keller and McKay, 1993). The optical effects of space weathering processes have principally three consequences on lunar soil spectra: overall reduction of the lunar soil reflectance, reduction of the absorption band depth, and increase of the continuum slope toward red wavelengths. If it is needed to acquire the natural mineralogical and chemical compositions of lunar soil in terms of its spectra, we should eliminate the optical effects of space weathering processes firstly.

The lunar surface is relatively simple in mineralogy, most lunar rocks are mineralogically dominated by feldspar, pyroxene, olivine and ilmenite (McKay et al., 1991; Zou Yongliao et al., 2004). The absorbance properties of these materials in the optical region are governed principally by electronic transitions due to ferrous iron, with a significant contribution from titanium (Burns, 1993). Most lunar rock types could be identified in terms of the type and abundance of mafic minerals that exhibit very diagnostic absorption features at between 0.6 μm and 2.5 μm. The main mineralogical characteristics of the lunar surface materials which could be identified by their reflectance spectra: the 0.75–1.1 μm spectral coverage is the location of the Fe^{2+} absorption band at 1 μm and the depth of the 0.9–1.0 μm absorption features is directly linked to the contents of ferrous and Fe-bearing silicate materials (Pieters et al., 1993; Charette and Adams, 1977).

2.2 Spectral parameters

In order to acquire the data on natural mineralogical and chemical compositions of lunar soil in terms of its spectra, we should eliminate the optical effects of space weathering processes firstly because the maturation process of lunar soils is known to make their spectra darker and redder. Hiroi et al. (1997) found there was a good linear correlation between continuum slope parameters and Is, where Is is the intensity of the ferromagnetic resonance from nanophase metallic iron particles (Morris et al., 1978). It means that a new method of determining FeO could be established based on their findings if the whole UV-VIS-NIR spectral data could be obtained (e.g. making use of the Clementine's UVVIS camera and NIR camera spectral data). However, the Clementine's NIR data have not yet been released to lunar workers because of the calibration problems.

Le Mouéic et al. (1999) proposed a useful reduction method of Clementine NIR data which used the calibrated UVVIS data as a reference for the determination of NIR data offsets. According to this useful reduction method, Le Mouéic et al. (2000) have established a new continuum slope parameter, Eq.(1), and the depth of 1-μm absorption feature, Eq.(2).

$$\text{slope} = \frac{R_{1500} - R_{750}}{(1.5 - 0.75)R_{750}}\ \mu\text{m}^{-1} \tag{1}$$

$$\text{depth } 1 = 1 - \frac{R_{950}}{(2.2/3)R_{750} + (0.8/3)R_{1500}} \tag{2}$$

where slope is the continuum slope; depth is the 1-μm absorption depth; R_{750}, R_{950} and R_{1500} are the reflectances at 750, 950, and 1500 nm, respectively.

They tested the correlation between the new parameter, Eq.(1), and Is on the basis of a broader set of lunar sample spectra, too. The lunar sample spectra were taken from Adams (1974) collections which could be downloaded in the Planetary Data System (PDS) mode. The results showed the continuum slope was correlated with Is for both lunar highland and mare materials and it provided an approach to reliable evaluation of the spectral alteration due to space weathering. They also investigated the relationship between the "slope" and the "depth 1" in a fresh crater measured at 2 km in diameter near the Aristarchus plateau, and fitted a linear equation "depth 1=-0.286 slope", which could eliminate the optical effects of space weathering processes successfully. They have established a new method of determining FeO

successfully, which is applied to the Aristarchus plateau (Le Mouéic et al., 2000), and the Tycho crater (Le Mouéic et al., 2002) on the basis of the Clementine NIR and UVUIS data.

3 The data

3.1 Multi-spectral images

The Clementine spacecraft has acquired the global-coverage and 11-band digital multi-spectral images of the Moon by using the ultraviolet-visible (UVVIS) camera and near-infrared (NIR) camera systems (Nozette et al., 1994; McEwen and Robinson, 1994). Both the cameras were chosen to develop mineralogical information about the lunar surface. The UVVIS camera has five filters from 415 to 1000 nm and its global 5-band (415, 750, 900, 950, and 1000 nm) UVVIS Digital Image Model (DIM) of the Moon at 100 m/pixel was released to the Planetary Data System (PDS) in 2000. Now, the U.S. Geological Survey (USGS) maintains the DIM of the Moon through the Map-A-Planet Web Site. A lot of excellent work has been done and wonderful achievements have been made by using the UVVIS dataset as described above.

However, because of a large varying dark frame signal and uncertainties involved in gain and offset values (Lucey et al., 1997, 1998a, b), the calibration problems have delayed the successful and immediate release of the Clementine NIR data set. The Clementine NIR data have six spectral bands (1100, 1250, 1500, 2000, 2600, and 2780 nm).

The U.S. Geological Survey endeavored to calibrate the Clementine NIR data set, and finished the radiometric and photometric corrections successfully. The USGS has released a reduced-resolution version of the Clementine near-infrared (NIR) mosaic which is processed to 500 m/pixel spatial resolution on the USGS Astrogeology Research Program Web Site. The NIR data have been radiometrically and geometrically controlled to the Clementine 750-nm mosaic, and photometrically normalized to form seamless, uniformly illuminated mosaics of the lunar surface. The first four NIR bands (1100–2000 nm) have also been normalized to reflectance based on the approach previously applied to the calibrated UVVIS global mosaics (Pieters, 1999). The 2600-nm and 2780-nm NIR bands are provided as the calibrated Clementine digital numbers (in counts/ms). Cahill et al. (2004) verified the quality and compatibility of the reduced-resolution version of Clementine NIR data

Table 1. Composition data for the lunar sampling sites used in this study (Blewett et al., 1997; Jolliff, 1999)

Site	FeO (wt%)	TiO_2 (wt%)	Site	FeO (wt%)	TiO_2 (wt%)
Apollo 11	15.8	7.5	Apollo 17-S1	17.8	9.6
Apollo 12	15.4	3.1	Apollo 17-S2	8.7	1.5
Apollo 14-LM	10.5	1.73	Apollo 17-S3	8.7	1.8
Apollo 14-Cone	10.3	1.6	Apollo 17-S5	17.7	9.9
Apollo 15-LM	15	1.9	Apollo 17-S6	10.7	3.4
Apollo 15-S1	16.8	1.6	Apollo 17-S7	11.6	3.9
Apollo 15-S2	11.5	1.3	Apollo 17-S8	12.3	4.3
Apollo 15-S4	16.6	1.2	Apollo 17-S9	15.4	6.4
Apollo 15-S6	12.1	1.5	Apollo 17-LRV1	16.3	8
Apollo 15-S7	13.9	1.1	Apollo 17-LRV2	13.4	4.4
Apollo 15-S8	15.2	1.7	Apollo 17-LRV3	14.8	5.5
Apollo 15-S9	16.9	1.8	Apollo17-LRV4/S2a	8.5	1.3
Apollo 15-S9a	20.4	2	Apollo 17-LRV5	9.8	2.6
Apollo 16-LM	5.6	0.6	Apollo 17-LRV6	10.3	2.6
Apollo 16-S1	5.4	0.6	Apollo 17-LRV7	16.1	6.8
Apollo 16-S2	5.5	0.6	Apollo 17-LRV8	15.7	6.6
Apollo 16-S4	4.6	0.5	Apollo 17-LRV9	14.6	6.1
Apollo 16-S5	5.9	0.7	Apollo 17-LRV10	11.2	3.7
Apollo 16-S6	6	0.7	Apollo 17-LRV11	12.7	4.5
Apollo 16-S8/S9	5.6	0.6	Apollo 17-LRV12	17.4	10
Apollo 16-S11	4.2	0.4	Luna 16	16.7	3.3
Apollo 16-S13	4.8	0.5	Luna 20	7.5	0.5
Apollo 17-LM	16.6	8.5	Luna 24	19.6	1

set, and they showed the data set is a reliable representation of the lunar surface with noise levels typically around 1%. All this means the NIR data set can be used to do some work pertaining to lunar surface science. The USGS is planning to release the full-resolution (200 m/pixel), multi-spectral files through the PDS Map-a-Planet Web Site in the future.

Owing to the need of combining the Clementine UVVIS data with the Clementine NIR data to accomplish our work, we acquire our appropriate image cube from the PDS Web Site (i.e., the Clementine UVVIS image cube from the Map-A-Planet Web Site and the Clementine NIR image cube from the USGS Astrogeology Research Program Web Site).

3.2 Lunar samples

Composition data for lunar soils are compiled in Table 1, which were derived from the studies of Blewett et al. (1997), Lucey et al. (2000a, b) and Jolliff (1999). There are 46 sampling sites and each site includes the contents of FeO and TiO_2. We localized the sampling sites on the basis of the studies of Lucey et al. (2000a, b).

4 Refinement of FeO mapping technique

Because Le Mouéic (1999, 2000, 2002) only reduced the Clementine NIR data set of local places on the lunar surface (e.g. Aristarchus plateau and Tycho crater), they have never dealt with the global NIR data. We have decided to use the Clementine UVVIS data and NIR data from the sampling sites to replace the corresponding lunar samples' spectra (i.e., using the bidirectional reflectance data to replace the corresponding directional hemispherical reflectance of lunar soils) (Liu Jian et al., 2005). Similar work was done by Blewett et al. (1997) firstly, and they used this technique to refine FeO mapping techniques described by Lucey et al. (1995) which had been developed in terms of the Clementine UVVIS data. Blewett et al. (1997) obtained very good results. At the same time, they made both localization studies and direct calibrations of FeO and TiO_2 algorithms relative to the Apollo and Luna sampling stations. The technique was also adopted by Jolliff (1999), Lucey et al. (1998a, b, 2000a, b), and Gills et al. (2003) successfully.

Although the spatial resolution (500 m/pixel) of UVVIS data and NIR data we used is lower than Blewett et al.'s (125 m/pixel), we still can practise this robust technique since Blewett et al. (1997) have utilized several pixels instead of a single pixel to represent the corresponding landing sites or sampling sites. According to Blewett et al. (1997), for the six early Apollo and Luna sites (Apollo 11, Apollo 12, Apollo 14, Luna 16, Luna 20, and Luna 24), a 11×11 pixel area was used to determine the reflectance values of the sampling sites, and for Apollo 15, 16, and 17, a 3×3 pixel was used to work out the average values for the separate stations.

We have obtained the spectra of 46 sampling sites from the Clementine UVVIS and NIR data (a pixel represents a site) firstly, as listed in Table 2. The accurate sampling sites have been localized, depending on the latitude/longitude information from the studies of Lucey et al. (2000a, b), Spudis and Pieters (1991), and Apollo Mission Reports (Wilhelms, 1987). We picked out the spectra of the Clementine images from all of the sampling sites singly, and then calculated the continuum slope parameter, Eq.(1), and the depth of 1-μm absorption, Eq.(2), respectively.

Le Mouéic et al. (2000, 2002) investigated the systematic relationships between the continuum slope and the 1-μm depth with different spectral alternation degrees on a small fresh crater (2 km in diameter) around the Aristarchus plateau located in lunar mare areas and another small fresh crater (1.2 km in diameter) around the Tycho crater located in lunar highland areas. Both the small fresh craters are homogenous areas. The "fresh" craters mean their maturity should change drastically and remarkably, and they are the ideal places to investigate the systematic relationships between the continuum slope and the 1-μm depth with different spectral alternation degreed. Their results showed the relationships between the continuum slope and the 1-μm depth with different spectral alternation degrees appears to be linear. The linear correlation (i.e., "depth 1=-0.286 slope") is adapted to both mare and highland soils. The resolution of the UVVIS and NIR data used by Le Mouéic et al. (2000, 2002) is 200 m/pixel, but our work depends on the 500 m/pixel data. We have investigated the relationship between the continuum slope and the 1-μm depth using the same fresh craters as Le Mouéic. However, the results are very unsatisfactory because there are only several pixels in the inner craters which represent the fresh areas. Owing to this situation, we used the parameter "depth 1=-0.286 slope" as the corresponding one in our work.

Le Mouéic et al. (2000, 2002) observed a good linear correlation between the continuum slope and the optical maturity parameter (OMAT) proposed by Lucey et al. (2000a, b). We have investigated the relationship between the continuum slope and the OMAT, too. However, the result (Fig. 1) is not awfully good and there does exist a poor correlation. We also fitted the relationship between the mafic iron sensitive parameter (depth 1+0.286 slope) and the bulk FeO content measured at the laboratory, the

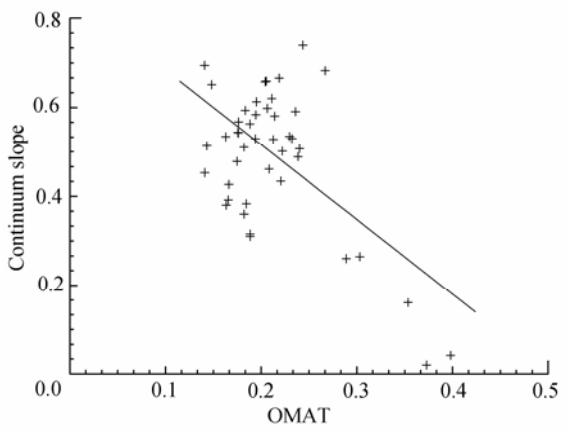

Fig. 1. Correlation between the continuum slope and the optical maturity parameter OMAT for all the sampling sites.

result is not so satisfactory (Fig. 2).

To reveal the reasons for the poor correlations between the continuum slope and the OMAT and between the mafic iron sensitive parameter and the bulk FeO content measured at the laboratory, we checked all the sampling sites carefully, but found that the poor correlations were not caused by inaccurate definition of the sampling locations. We examined the spectra of all the sampling sites and plotted the spectra of all the sampling sites carefully. In order to observe their absorption response clearly, we conducted a continuum removal toward the spectra of each sampling site. According to our observations, only about half of the sampling sites yielded normal spectra, which can be used to refine the method developed by Le Mouéic et al. (2000, 2002). These normal sampling sites include Apollo 14-Cone, Apollo 15-LM, Apollo 15-S1, Apollo 15-S4, Apollo 15-S7, Apollo 15-S8, Apollo 15-S9, Apollo 16-S2, Apollo 16-S6, Apollo 16-S8/S9, Apollo 16-S11, Apollo 16-S13, Apollo 17-S2, Apollo 17-S3, Apollo 17-S5, Apollo 17-S6, Apollo 17-S7, Apollo 17-S8, Apollo 17-LRV3, Apollo17-LRV4/S2a, Apollo 17-LRV6, Apollo 17-LRV7, Apollo 17-LRV10, Apollo 17-LRV11, and Luna 20, totaling 25 sampling sites. The spectra of Apollo 15-S7 are shown in Fig. 3a and the continuum removal spectra in Fig. 3b. From Fig. 3a and b, we can see that both the 750 nm and 1500 nm filters are really the left and right shoulders of Eq.(1) and Eq.(2) and can be used to evaluate the depth of the 1-μm absorption feature accurately. Because the spectra of the rest normal sites are similar to those of Apollo 15-S7, there is no need to say more here.

However, there still are many exceptional sampling sites whose right shoulders (1500 nm filter) of Eq.(1) and Eq.(2) could not be used to evaluate the depth at which the 1-μm absorption feature appears accurately. In order to reveal the reason why the spectra of these sampling sites are not suitable to Eq.(1) and Eq.(2), we took Lunar 16 for example, as shown in Fig. 3c and d. From Fig. 3c, it is seen that there is a weak absorption band at 1500 nm. From Fig. 3d, it is observed that the continuum removal spectral reflectance of the 1500 nm filter is less than that of the 1250 nm filter, which means that the 1500nm filter is not suitable to be the right shoulder to evaluate the depth of the 1-μm absorption feature. From the spectra of Luna 16, it can also be concluded that Eq.(1) and Eq.(2) are not the appropriate spectral parameters for the sites or places similar to Luna 16. In these sites or places, if we use the 1250 nm filter as the right shoulder of the 1-μm absorption feature to evaluate the depth of the 1-μm absorption feature, the accuracy could be higher than that in case the 1500 nm filter is used. The spectra of the rest abnormal sites are similar to those of Luna 16 and they are all exceptional. Because we could not use Eq.(1) and Eq.(2) to evaluate the depth of 1-μm feature accurately, first and for most, we should remove these sites from the normal sites.

After discarding 21 abnormal sampling sites, we utilized the spectra of the rest 25 sampling sites to do

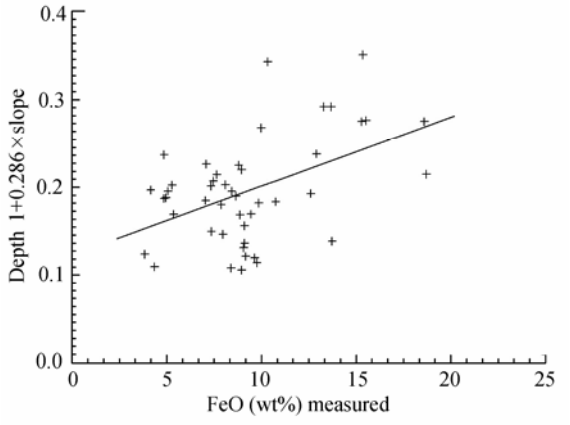

Fig. 2. Correlation between the mafic iron parameter and the measured FeO values for all the sampling sites.

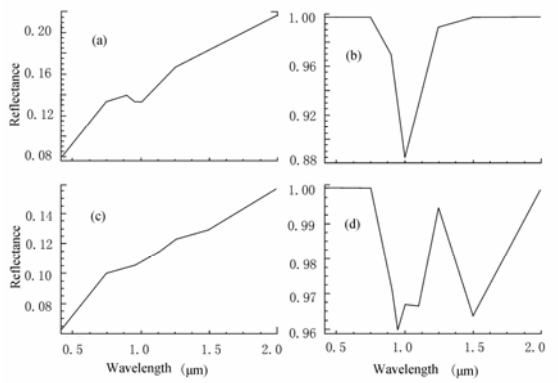

Fig. 3. The spectral profiles of Apollo 15-S7 and Luna 16. (a) The spectral profile of Apollo 15-S7; (b) the spectral profile of Apollo 15-S7 obtained after continuum removal; (c) the spectral profile of Luna 16; and (d) the continuum removal spectral profile of Luna 16.

refining work again. We investigated the relationship between the continuum slope and the OMAT again, which is vital to illustrate the removal of maturity. The result is shown in Fig. 4 and the correlation is much better linear than that shown in Fig. 1. The good correlation illuminates that the continuum slope Eq.(1) could be used to eliminate the optical effects of space weathering processes in our work. We also investigated the correlation between the "depth 1+0.286 slope" and the bulk FeO content in terms of the data from the same sampling sites. The result is shown in Fig. 5, where the correlation is much better linear than that shown in Fig. 2, too. The good correlation ensures that this set of data can be used to refine the FeO mapping method.

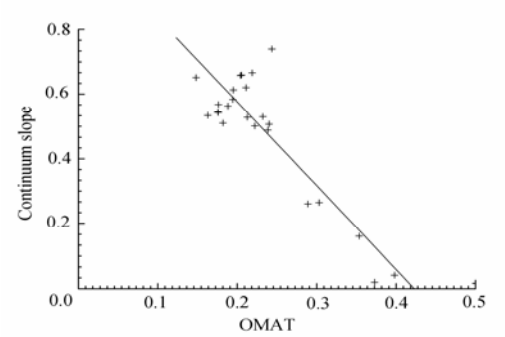

Fig. 4. Correlation between the continuum slope and the optical maturity parameter OMAT for the suitable sampling sites.

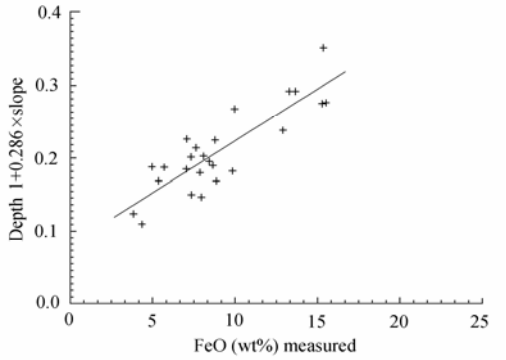

Fig. 5. Correlation between the mafic iron parameter and the measured FeO values for the suitable sampling sites.

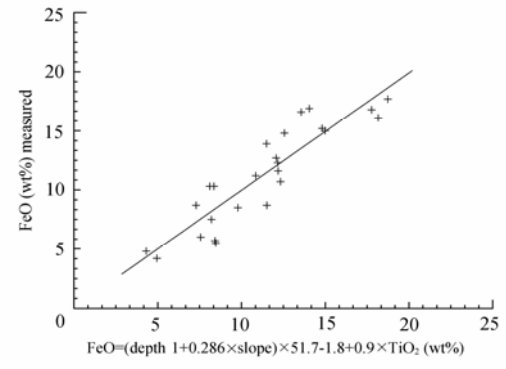

Fig. 6. Total FeO contents estimated from Eq.(3) versus the measured contents.

Because our method can be used to evaluate mafic FeO in the lunar soils, but can not be used to evaluate the FeO in correlation with ilmenite we want to acquire the total FeO content by adding 0.9 TiO_2 (wt%) to the weight percent of mafic FeO in our mafic iron evaluation as Le Mouéic et al. (2000, 2002) did. According to the normal sampling sites, we established our own FeO mapping equation, i.e., Eq.(3).

$$\mathrm{FeO_{Total}(wt\%)=FeO_{mafic}+FeO_{ilmenite}} = 51.7\times(\mathrm{depth}\ 1+0.286\times\mathrm{slope})-1.8+0.9\mathrm{TiO_2} \quad (3)$$

In order to test Eq.(3)'s robust, we investigated the correlation between the FeO contents from the corresponding sampling sites as computed by Eq.(3) and the FeO contents measured at the laboratory. The acquired correlation coefficient is 0.91, which means there is a good correlation between predicted FeO and measured FeO. The good correlation (Fig. 6) demonstrates that it is possible to evaluate mafic iron in the location whose 750 nm filter and 1500 nm filter could be used to evaluate the depth of the 1-μm absorption feature with this algorithm. The difference between predicted FeO and measured FeO measured shows a standard deviation of 1.8 wt%. If the full-resolution Clementine NIR data could be used in the future, we will obtain a correlation coefficient better than 0.91.

When the full-resolution Clementine NIR data or other new NIR data are released, we may perfect our refined method [Eq.(3)]. Till that time, it will be possible to use both the FeO mapping methods to evaluate FeO of the global lunar surface.

5 Conclusions

We have used the Clementine UVVIS and NIR dataset of the lunar sampling sites to replace the directional-hemispherical spectra of lunar soils, as done by Blewett et al. (1997) for the method developed by Lucey et al. The technique can be used of refine the FeO mapping method of Le Mouéic et al. (2000, 2002). Our original aim was to refine it only. However, when we applied the technique to refining the FeO mapping method, we found that many abnormal sampling sites are not suitable to Eqs.(1) and (2) Le Mouéic et al. which were used to evaluate the depth of 1-μm feature accurately. The main reason why these sampling sites are defined as "unsuitable" is that there is an absorption in the 1500 nm filter, and we can not utilize the 1500 nm filter as the right shoulder to evaluate the depth of 1-μm feature under these situations. After excluding the 21 sampling sites from our work, we used the rest sites to refine the

mapping technique. The results are very satisfactory and we has established our own FeO mapping equation, Eq.(3) which is applicable to the places whose 1500 nm filter could be used as the right shoulder to evaluate the depth at which the 1-μm feature appears accurately. In our work we have also acquired some useful experiences in scientific applications of our own dataset of the Chang'E-1 mission.

Acknowledgements This research is supported by the National Natural Science Foundation of China (Grant No. 40373037).

References

Adams J.B. (1974) Visible and near-infrared diffuse reflectrance spectra of pyroxenes as applies to remote sensing of solid bodies in the solar system [J]. *J. Geophys. Res*. **79**, 4829.

Blewett D.T., Lucey P.G., Hawke B.R., and Jolliff B.L. (1997) Clementine images of the lunar sample-return stations: Refinement of FeO and TiO_2 mapping techniques [J]. *J. Geophys. Res*. **102**, 16319–16325.

Burns R.G. (1993) Origin of electronic spectra of minerals in the visible to near-infrared region. In *Remote Geochemical Analysis* [M]. pp.3–29. Cambridge University Press, New York.

Cahill J.T. et al. (2004) Verification of quality and compatibility for the newly calibrated Clementine NIR Data Set. In *Lunar and Planet. Sci. Conf.* [C]. **XXXV**, 1469.

Charette M.P. and Adams J.B. (1977) Spectral reflectance of lunar highland rocks. In *Proc. Luar Sci. Conf. 8th* [C]. 172.

Fischer E.M. and Pieters C.M. (1994) Remote determination of exposure degree and iron concentration of lunar soils using VIS-NIR spectral methods [J]. *Icarus*. **111**, 475.

Fischer E.M. and Pieters C.M. (1996) Composition and exposure age of the Apollo 16 Cayley and Descartes regions from Clementine data: Normalizing the optical effects of space weathering [J]. *J. Geophys. Res*. **101**, 2225.

Gills J.J. et al. (2003) A revised algorithm for calculation TiO_2 concentrations from Clementine UVVIS data: A synthesis of rock, soil, and remotely sensed TiO_2 concentrations. [J]. *J. Geophys. Res*. **108**, 5009.

Hapke B. et al. (1975) Effects of vapor-phase deposition processes on the optical, chemical, and magnetic properties of the lunar regolith [J]. *Moon*. **13**, 339.

Haskin L. and Warren P. (1991) Lunar chemistry. In *Lunar Source Book—A User's Guide to the Moon* [M]. pp.357–474. Cambridge University Press, New York.

Hiroi T. et al. (1997) New considerations for estimating lunar soil maturity from VIS-NIR reflectance spectroscopy. In *Lunar and Planetary Science Conf.* [C]. **XXVII**, 575.

Jolliff B.L. (1999) Clementine UVVIS multispectral data and the Apollo 17 landing site: What can we tell and how well [J]. *J. Geophys. Res*. **104**, 148.

Keller L.P. and McKay D.S. (1993) Discovery of vapor deposits in the lunar regolith [J]. *Science*. **261**, 1305.

Le Mouéic S. et al. (1999) A new data reduction approach for the Clementine NIR data set: Application to Aristillus, Aristarchus, and Kepler [J]. *J. Geophys. Res*. **104**, 3833.

Le Mouéic S. et al. (2000) Discrimination between maturity and composition of lunar soils from integrated Clementine UV-visible/near-infrared data Application to the Aristarchus Plateau [J]. *J. Geophys. Res*. **105**, 9445.

Le Mouéic S. et al. (2002) Calculating iron contents of lunar highland materials surrounding Tycho crater from integrated Clementine UV-visible and near-infrared data [J]. *J. Geophys. Res*. **107**, 5074.

Liu Jian, Ouyang Ziyuan, Li Chunlai, and Zou Yongliao (2005) Advances in the study of lunar opposition effect [J]. *Chinese Journal of Geochemistry*. **24**, 173–178.

Lucey P.G. et al. (1995) Abundance and distribution of iron on the Moon [J]. *Science*. **268**, 1150.

Lucey P.G. et al. (1998a) Mapping the FeO and TiO_2 content of the lunar surface with multispectral imagery [J]. *J. Geophys. Res*. **103**, 3679.

Lucey P.G. et al. (1998b) Calibration of the Clementine near infrared camera: Ready for prime time. In *Lunar and Planetary Science Conf.* [C]. **XXXI**, 1576.

Lucey P.G. et al. (1997) Progress toward calibration of the Clementine NIR Camera Data Set. In *Lunar and Planetary Science Conf.* [C]. **XXVII**, 843.

Lucey P.G. et al. (2000a) Lunar iron and titanium abundance algorithms based on final processing Clementine UVVIS images [J]. *J. Geophys. Res*. **105**, 20297.

Lucey P.G. et al. (2000b) Imaging of lunar surface maturity [J]. *J. Geophys. Res*. **105**, 20377.

McKay D.S. et al. (1991) The Lunar Regolith. In *Lunar Source Book—A User's Guide to the Moon* [M]. pp.285–356. Cambridge University Press, New York.

McKay D.S. et al. (1974) Grain size and the evolution of lunar soils. In *Proc. Lunar Sci. Conf. 5th* [C]. 887.

McEwen A.S. and Robinson E. (1994) Clementine observations of the Aristarchus Region of the Moon [J]. *Science*. **266**, 1858.

Morris R.V. et al. (1978) The surface exposure/maturity of lunar soils—Some concepts and Is/FeO compilation. In *Proc. Luar Sci. Conf. 9th* [C]. 2287.

Nozette S. et al. (1994) The Clementine mission to the Moon—Scientific overview [J]. *Science*. **266**, 1835.

Pieters C. M. et al. (1993) *Remote Geochemical Analysis* [M]. Cambridge University Press, New York.

Pieters C.M. (1999) *The Moon as a Spectral Calibration Standard Enabled by Lunar Samples: The Clementine Example* [C]. pp.8025. Arizona, Flagstaff.

Shkuratov Y.G. et al. (1999) Iron and titanium abundance and maturity degree distribution on the lunar nearside [J]. *Icarus*. **137**, 222.

Shkuratov Y.G. et al. (2003) Estimates of the lunar surface composition with Clementine images and LSCC data. In *Lunar and Planetary Science Conf.* [C]. **XXXIV**, 1258.

Spudis P.D. and Pieters C.M. (1991) *Lunar Source Book—A User's Guide to the Moon* [M]. Cambridge University Press, New York.

Taylor R.S. (1987) The unique lunar composition and its bearing on the origin of the moon [J]. *Geochim. Cosmochim. Acta*. **51**, 1297.

Wilhelms D.E. (1987) *The Geologic History of the Moon* [M]. USGS Prof. Pap. 1348.

Xu Tao, Ouyang Ziyuan, Li Chunlai, and Xu Lin (2005) Advance in lunar exploration detectors [J]. *Chinese Journal of Geochemistry*. **24**, 95–100.

Zou Yongliao et al. (2004) Reflectivity of the lunar surface materials [J]. *Chin. J. Astron. Astrophys*. **4**, 97.